Inorganic Chemistry

pubs.acs.org/IC

Communication

$Na_3Bi(IO_3)_6$: An Alkali-Metal Bismuth Iodate with Intriguing One-Dimensional $[BiI_6O_{18}]$ Chains and Pressure-Induced Structural Transition

Huimin Song,[†] Dequan Jiang,[†] Naizheng Wang, Wenhao Xing, Ruixin Guo, Zheshuai Lin, Jiyong Yao, Yonggang Wang,* Heng Tu,* and Guochun Zhang

Cite This: *Inorg. Chem.* 2021, 60, 2893−2898

ABSTRACT: An alkali-metal bismuth iodate, $Na_3Bi(IO_3)_6$, was successfully obtained by the hydrothermal method for the first time and contains intriguing one-dimensional $[BiI_6O_{18}]$ chains. High-pressure Raman spectra were carried out to investigate the structural transition of $Na_3Bi(IO_3)_6$. Electronic states and anisotropic optical responses were also investigated by theoretical calculations.

Iodates(V) possess abundant structural diversity because of stereochemically active lone-pair electrons.[1−4] In iodates(V), I^{5+} cations usually adopt three- or four-coordinated environments to form the $[IO_3]$ or $[IO_4]$ fundamental unit. Furthermore, $[IO_3]$ and $[IO_4]$ units can be isolated or connected with each other, which results in the formation of other various units such as $[I_2O_5]$ and $[I_3O_8]$.[5−10] Additionally, iodates(V) generally possess high optical anisotropy, which can influence multiple properties, such as second harmonic generation (SHG), piezoelectricity, birefringence, and photocatalysis.[11−15] In recent years, a series of excellent iodates with the above functions have been found, including $LiM^{II}(IO_3)_3$ (M^{II} = Zn, Cd, Mg), $ABi_2(IO_3)_2F_5$ (A = NH_4, K, Rb, Cs), $Y(IO_3)_3$, and MIO_3F (M = Zn, Cd).[16−22]

Combining various structural units into one compound is an effective strategy for enhancing the performance of functional materials through the synergistic effect between structural units.[23−26] Similar with I^{5+} cations, Bi^{3+} cations also contain lone-pair electrons. Therefore, introducing Bi^{3+} cations into iodates can further modulate the functional properties.[27] Several multifunctional materials have been discovered in bismuth iodates.[28−30] For example, $BiIO_4$, a new type of polar material, not only exhibits a large SHG response but also displays high photocatalytic activities for reactive oxygen species generation and CO_2 reduction because the large macroscopic polarization originates from Bi^{3+} and I^{5+} cations.[31−33]

Pressure, as an important thermodynamic parameter, has always been an effective tool for modulating the crystal structure and inducing interesting transitions in the structures and properties.[34−36] High pressure generally can reduce the distance between atoms in a controllable way, resulting in the discovery of hidden phenomena in materials.[37−40] Up to now, only four iodates, i.e., $LiIO_3$, KIO_3, $AgIO_3$, and $Fe(IO_3)_3$, have been investigated under the condition of high pressure,[41−45] which prompted us to further investigate the high-pressure behavior of iodates.

In order to increase the band gap and obtain high-transmittance optical anisotropy materials, we introduce alkali metals into bismuth iodates. A new iodate with a novel structural feature, $Na_3Bi(IO_3)_6$, was obtained by the hydrothermal method. The pressure-induced structural transition was investigated for the first time. Thermal analysis, IR, Raman, and UV−vis diffuse-reflectance spectra, and theoretical calculations were performed to further understand the structure−property relationships.

Submillimeter pale-yellow single crystals of $Na_3Bi(IO_3)_6$ were obtained by the hydrothermal method (the experimental details are shown in the Supporting Information). The purity of the sample was verified by powder X-ray diffraction (XRD) analysis, as shown in Figure 1a. The experimental powder XRD pattern was well-consistent with the simulated one based on the single-crystal crystallographic data. Energy-dispersive X-ray spectroscopy (EDS) analysis (Figure S1) confirmed the

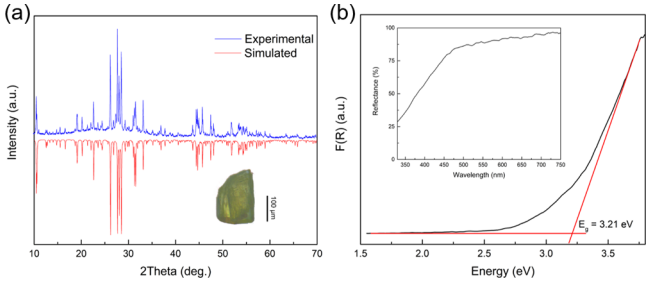

Figure 1. (a) Powder XRD patterns and (b) experimental band gap of $Na_3Bi(IO_3)_6$.

Received: December 18, 2020
Published: February 11, 2021

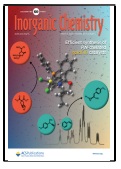

https://dx.doi.org/10.1021/acs.inorgchem.0c03697
Inorg. Chem. 2021, 60, 2893−2898

presence of Na, Bi, and I atoms, and the molar ratio of Na/Bi/I (3.88:1.09:5.52) was comparable to the stoichiometric ratio, which verified the correctness of the single-crystal XRD analysis.

$Na_3Bi(IO_3)_6$ crystallizes in the triclinic $P\bar{1}$ space group with cell parameters of a = 7.2013(2) Å, b = 8.9076(2) Å, c = 14.5054(3) Å, α = 105.441(2)°, β = 94.536(2)°, and γ = 99.331(2)°. The detailed crystal data of $Na_3Bi(IO_3)_6$ are listed in Tables S1–S3. A total of 1 unique Bi, 3 unique Na, 6 unique I, and 18 unique O atoms constitute its asymmetric unit. All atoms are located on the general *Wyckoff* position 2*i*. Every I atom is bonded with three O atoms to build a $[IO_3]$ unit with I–O bond lengths in the range of 1.780(5)–1.850(5) Å, which match well with the previously reported values (Figure 2a).[2,33]

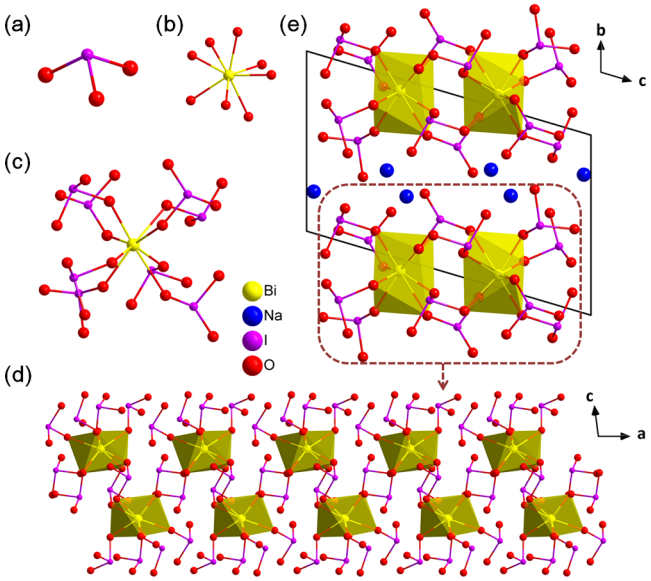

Figure 2. (a) $[IO_3]$ unit, (b) $[BiO_8]$ polyhedron, (c) $[BiI_8O_{24}]$ group, (d) $[BiI_6O_{18}]$ chain, and (e) unit cell of $Na_3Bi(IO_3)_6$.

The Bi atoms are eight-coordinated, with O atoms forming distorted $[BiO_8]$ polyhedra with Bi–O bond lengths ranging from 2.279(5) to 2.802(7) Å (Figure 2b). Each $[BiO_8]$ polyhedron connects with eight $[IO_3]$ units by corner-sharing O atoms, forming the $[BiI_8O_{24}]$ group (Figure 2c). Furthermore, neighboring $[BiI_8O_{24}]$ groups polymerize by sharing $[IO_3]$ units to generate the one-dimensional (1D) $[BiI_6O_{18}]$ chains (Figure 2d). All of the Na atoms are bonded to six O atoms to build $[NaO_6]$ polyhedra (Figure S2a). $[NaO_6]$ polyhedra connect with each other by corner- or edge-sharing O atoms to form 1D $[Na_3O_{13}]$ chains (Figure S2b,c). 1D $[BiI_6O_{18}]$ and $[Na_3O_{13}]$ chains connect by sharing O atoms to form a three-dimensional structure (Figure 2e). The valence states of all atoms were calculated according to the bond valence sum, and the results are in good agreement with the theoretical ones (Table S2).[46]

In order to further understand the structural relationships between $Na_3Bi(IO_3)_6$ and other alkali-metal bismuth iodates, the structures with the molecular formula of $M_xBi(IO_3)_{3+x}$ (M = alkali metal; x is an integer) are summarized in Table S4. The bond length of Bi–O is limited to less than 2.81 Å and the bond length of I–O is limited to less than 2.30 Å based on refs 47–49. The molecular formula of $M_xBi(IO_3)_{3+x}$ can be recognized as the combination of $M_x(IO_3)_x$ and $Bi(IO_3)_3$. As can be seen from Table S4, when the values of x are 0 and 1, the compounds possess 2D $[BiI_3O_9]$ and $[BiI_4O_{12}]$ layers, and the molar ratios of M/(Bi + I) are only 0 and 1/5, respectively. The small amount of alkali metal could not break the polymerization of [BiIO] groups, which tend to form 2D layers (Figure S3). With increasing x, the dimensionality of the [BiIO] group begins to decrease. When x = 2 and 3, the corresponding compounds contain 1D $[BiI_5O_{15}]$ and $[BiI_6O_{18}]$ chains, respectively (Figures S3 and 2). The molar ratio of M/(Bi + I) for $Na_3Bi(IO_3)_6$ is up to 3/7. It can be speculated that $M_xBi(IO_3)_{3+x}$ may have 0D [BiIO] cluster structures as the value of x is increased to a certain extent.

IR and Raman spectra were measured to understand the microscopic coordination information on $Na_3Bi(IO_3)_6$ (Figure S4). The sharp absorption peaks at 825, 787, 753, and 677 cm^{-1} in the IR spectrum and 822, 803, 790, 761, 753, 711, 685, and 668 cm^{-1} in the Raman spectrum are assigned to the asymmetric (ν_3) and symmetric (ν_1) stretching vibrations of the $[IO_3]$ units. The peaks at 422 cm^{-1} in the IR spectrum and 419 cm^{-1} in the Raman spectrum are attributed to the Bi–O vibrations. The results of the IR and Raman spectra confirm the existence of Bi–O bonds and $[IO_3]$ units in the structure of $Na_3Bi(IO_3)_6$, which is consistent with the single-crystal XRD data.

In order to investigate the structural changes of $Na_3Bi(IO_3)_6$ under high pressure, high-pressure Raman spectra were carried out. On the basis of the above IR and Raman spectra, the vibrations of $[IO_3]$ units concentrate in the range of 650–850 cm^{-1}, high-pressure Raman spectra and Raman shift versus pressure in this range are shown in Figure 3, and Raman

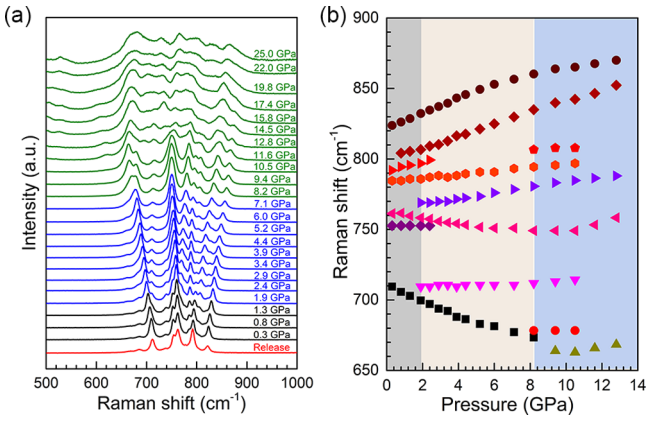

Figure 3. (a) High-pressure Raman spectra and (b) Raman shift versus pressure of $Na_3Bi(IO_3)_6$.

vibrational modes (ν_1 and ν_3) of the $[IO_3]$ units are displayed in Figure S5. The Raman spectrum under 0.3 GPa is in agreement with that under ambient pressure. It is obvious that most of the Raman peaks move to high wavenumbers with an increase of the pressure, which implies that most I–O bonds are compressed. However, the Raman peaks at 761 and 709 cm^{-1} move to low wavenumbers. This phenomenon indicates that there are elongated I–O bonds in the $[IO_3]$ units, which can also be found in the high-pressure investigation of $Fe(IO_3)_3$.[45] With increasing pressure to 1.9 GPa, two new Raman peaks are emerged at 769 and 709 cm^{-1}, respectively. Besides, Raman peaks at 797 and 752 cm^{-1} disappeared in the following compression process. The appearance of new peaks and the disappearance of existing peaks in this pressure point

https://dx.doi.org/10.1021/acs.inorgchem.0c03697
Inorg. Chem. 2021, 60, 2893–2898

imply that the original $[IO_3]$ vibrational mode is changed. Because the pressure regulates the I−O bond lengths in the $[IO_3]$ units, which leads to most I−O bonds being shortened and a few I−O bonds being elongated, the original configurations of the $[IO_3]$ units are broken and new distorted $[IO_3]$ units are formed. The change of the $[IO_3]$ units further influences the crystal structure, which implies that a new phase II is formed at 1.9 GPa. When the pressure reaches up to 8.2 GPa, a new change appears. The Raman peak at 673 cm^{-1} splits into two peaks, and a new peak emerges at 806 cm^{-1}. This phenomenon indicates that the $[IO_3]$ units further distort under higher pressure, and a new phase transition occurs. As the pressure further increases, all Raman peaks move to high wavenumbers, which indicates that all of the $[IO_3]$ units are compressed in the following process. In the previous reports,[42,45] the lone-pair electrons of I^{5+} cations are gradually suppressed and the coordination numbers are increased under compression. Thus, in the new phase III, the $[IO_3]$ units have a trend of combining with neighboring O atoms to generate new $[IO_x]$ (x = 4, 5, or 6) units in the following compression. Overall, during the whole compression process, the [IO] vibrational mode is altered twice, which implies that it experiences two structural phase transitions, phases II and III. Besides, as the pressure releases to ambient pressure, the Raman spectrum also returns, indicating that $Na_3Bi(IO_3)_6$ has undergone reversible phase transitions. Further structural characterization under pressure is in progress.

The thermal behavior of $Na_3Bi(IO_3)_6$ was observed by thermal gravimetric (TG) and differential scanning calorimetric (DSC) analysis. $Na_3Bi(IO_3)_6$ has a relatively high thermal stability of up to 400 °C (Figure S6). Three obvious endothermic peaks appeared at 431, 556, and 654 °C, respectively. From 420 to 870 °C, the total mass loss was 75.9%, accounting for the decomposition process of three molecules of I_2O_5, which is consistent with the calculated value of 75.4%. The band gap of $Na_3Bi(IO_3)_6$ was estimated by UV−vis diffuse-reflectance spectroscopy. As shown in Figure 1b, the experimental band gap is 3.21 eV, which is comparable to that of the previously reported bismuth iodates.[30,48]

To better understand the structure−property relationships of $Na_3Bi(IO_3)_6$, first-principles calculations were carried out. Calculations indicate that $Na_3Bi(IO_3)_6$ possesses an indirect band gap with a value of 3.34 eV (Figure S7), which is slightly higher than the experimental value of 3.21 eV. Compared with other iodates (Table S4), its calculated band gap was overestimated, and the reasons will be further investigated. The density of states (DOS) and partial density of states (PDOS) of $Na_3Bi(IO_3)_6$ are shown in Figure 4a. It is obvious that the valence band maximum is mainly derived from the O 2*p* orbital and the conduction band minimum is mostly composed of I 5*s*5*p* and O 2*p* orbitals with a small amount of mixing of the Bi 6*p* orbital. The results imply that I−O and Bi−O bonds have an important role in the optical properties of $Na_3Bi(IO_3)_6$.

The refractive index is generally deemed to be a major parameter to assess the optical anisotropy of compounds. The refringence at different wavelengths of $Na_3Bi(IO_3)_6$ is shown in Figure 4b using the first-principles calculations. It is found that $Na_3Bi(IO_3)_6$ is a negative biaxial optical crystal and has a relatively large birefringence, which is 0.13 at 800 nm. To trace the source of the refractive index, the electron location function (ELF) of the I^{5+} and Bi^{3+} cations is displayed in Figure 4c. The contributions of the $[BiO_8]$ and $[IO_3]$ units to

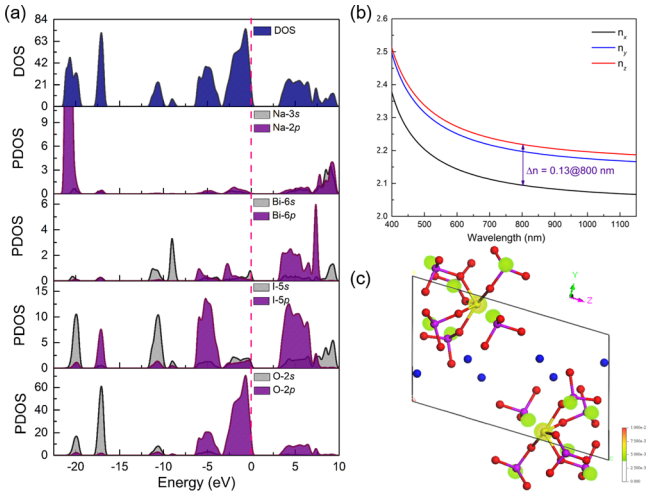

Figure 4. (a) PDOS and total DOS, (b) calculated refractive index, and (c) ELF of $Na_3Bi(IO_3)_6$.

the birefringence are calculated to be 0.03 and 0.07 at 800 nm, respectively (Figure S8). It was found that the synergistic effect of lone-pair electrons on I^{5+} and Bi^{3+} cations leads to the anisotropy of the electronic distribution, which finally generates a large birefringence in $Na_3Bi(IO_3)_6$.

In conclusion, a new alkali-metal bismuth iodate, $Na_3Bi(IO_3)_6$, with intriguing 1D $[BiI_6O_{18}]$ chains was successfully obtained by the hydrothermal reaction. The structures with the molecular formula of $M_xBi(IO_3)_{3+x}$ (M = alkali metal) were investigated, and it was shown that, with an increase of the molar ratio of M/(Bi + I), the dimensionality of $M_xBi(IO_3)_{3+x}$ decreases. High-pressure Raman spectra implied that $Na_3Bi(IO_3)_6$ went through two reversible phase transitions caused by changes of the $[IO_3]$ vibrational mode. First-principles calculations demonstrated that $Na_3Bi(IO_3)_6$ had a relatively large birefringence Δn = 0.13 at 800 nm. This work enriches the structural diversity of iodate chemistry and provides a new strategy for exploring novel functional materials under the condition of high pressure.

■ ASSOCIATED CONTENT

Supporting Information

The Supporting Information is available free of charge at https://pubs.acs.org/doi/10.1021/acs.inorgchem.0c03697.

Experimental and computational details, crystal data, crystal structural discussions, EDS analysis, IR and Raman spectra, TG−DSC curves, and calculated figures of $Na_3Bi(IO_3)_6$ (PDF)

Accession Codes

CCDC 2046288 contains the supplementary crystallographic data for this paper. These data can be obtained free of charge via www.ccdc.cam.ac.uk/data_request/cif, or by emailing data_request@ccdc.cam.ac.uk, or by contacting The Cambridge Crystallographic Data Centre, 12 Union Road, Cambridge CB2 1EZ, UK; fax: +44 1223 336033.

■ AUTHOR INFORMATION

Corresponding Authors

Yonggang Wang − *Center for High Pressure Science and Technology Advanced Research, Beijing 100094, China;* orcid.org/0000-0003-4816-9182;
Email: yonggang.wang@hpstar.ac.cn

https://dx.doi.org/10.1021/acs.inorgchem.0c03697
Inorg. Chem. 2021, 60, 2893−2898

Heng Tu − *Beijing Center for Crystal Research and Development, Key Laboratory of Functional Crystals and Laser Technology, Technical Institute of Physics and Chemistry, Chinese Academy of Sciences, Beijing 100190, China; Center of Materials Science and Optoelectronics Engineering, University of Chinese Academy of Sciences, Beijing 100049, China;* orcid.org/0000-0003-2871-1800; Email: tuheng@mail.ipc.ac.cn

Authors

Huimin Song − *Beijing Center for Crystal Research and Development, Key Laboratory of Functional Crystals and Laser Technology, Technical Institute of Physics and Chemistry, Chinese Academy of Sciences, Beijing 100190, China; Center of Materials Science and Optoelectronics Engineering, University of Chinese Academy of Sciences, Beijing 100049, China;* orcid.org/0000-0002-2329-0704

Dequan Jiang − *Center for High Pressure Science and Technology Advanced Research, Beijing 100094, China;* orcid.org/0000-0003-0998-5507

Naizheng Wang − *Beijing Center for Crystal Research and Development, Key Laboratory of Functional Crystals and Laser Technology, Technical Institute of Physics and Chemistry, Chinese Academy of Sciences, Beijing 100190, China; Center of Materials Science and Optoelectronics Engineering, University of Chinese Academy of Sciences, Beijing 100049, China;* orcid.org/0000-0002-2688-0400

Wenhao Xing − *Beijing Center for Crystal Research and Development, Key Laboratory of Functional Crystals and Laser Technology, Technical Institute of Physics and Chemistry, Chinese Academy of Sciences, Beijing 100190, China; Center of Materials Science and Optoelectronics Engineering, University of Chinese Academy of Sciences, Beijing 100049, China;* orcid.org/0000-0003-1258-419X

Ruixin Guo − *Beijing Center for Crystal Research and Development, Key Laboratory of Functional Crystals and Laser Technology, Technical Institute of Physics and Chemistry, Chinese Academy of Sciences, Beijing 100190, China; Center of Materials Science and Optoelectronics Engineering, University of Chinese Academy of Sciences, Beijing 100049, China*

Zheshuai Lin − *Beijing Center for Crystal Research and Development, Key Laboratory of Functional Crystals and Laser Technology, Technical Institute of Physics and Chemistry, Chinese Academy of Sciences, Beijing 100190, China; Center of Materials Science and Optoelectronics Engineering, University of Chinese Academy of Sciences, Beijing 100049, China;* orcid.org/0000-0002-9829-9893

Jiyong Yao − *Beijing Center for Crystal Research and Development, Key Laboratory of Functional Crystals and Laser Technology, Technical Institute of Physics and Chemistry, Chinese Academy of Sciences, Beijing 100190, China; Center of Materials Science and Optoelectronics Engineering, University of Chinese Academy of Sciences, Beijing 100049, China;* orcid.org/0000-0002-4802-5093

Guochun Zhang − *Beijing Center for Crystal Research and Development, Key Laboratory of Functional Crystals and Laser Technology, Technical Institute of Physics and Chemistry, Chinese Academy of Sciences, Beijing 100190, China; Center of Materials Science and Optoelectronics Engineering, University of Chinese Academy of Sciences, Beijing 100049, China; State Key Laboratory of Crystal Materials, Shandong University, Jinan 250100, China;* orcid.org/0000-0002-8795-6130

Complete contact information is available at: https://pubs.acs.org/10.1021/acs.inorgchem.0c03697

Author Contributions

†These authors contributed equally.

Notes

The authors declare no competing financial interest.

■ ACKNOWLEDGMENTS

This work was financially supported by the National Natural Science Foundation of China (Grants 51972314 and 51890865) and National Key R&D Program of China (Grants 2016YFB0402103 and 2016YFB1102301).

■ REFERENCES

(1) Li, Y. H.; Wu, H. P.; Zhang, B. B.; Yang, Z. H.; Han, G. P.; Pan, S. L. Mo^{6+} Cation Enrichment of the Structure Chemistry of Iodates: Syntheses, Structures, and Calculations of $Ba(MoO_2)_2(IO_3)_4O$, $Ba_3[(MoO_2)_2(IO_3)_4O(OH)_4]\cdot 2H_2O$, and $Sr[(MoO_2)_6(IO_4)_2O_4]\cdot H_2O$. *Inorg. Chem.* **2018**, *57*, 9376−9384.

(2) Zhang, M.; Su, X.; Mutailipu, M.; Yang, Z. H.; Pan, S. L. $Bi_3OF_3(IO_3)_4$: Metal Oxyiodate Fluoride Featuring a Carbon-Nanotube-like Topological Structure with Large Second Harmonic Generation Response. *Chem. Mater.* **2017**, *29*, 945−949.

(3) Hu, C. L.; Mao, J. G. Recent advances on second-order NLO materials based on metal iodates. *Coord. Chem. Rev.* **2015**, *288*, 1−17.

(4) Qian, Z.; Wu, H. P.; Yu, H. W.; Hu, Z. G.; Wang, J. Y.; Wu, Y. C. New polymorphism for $BaTi(IO_3)_6$ with two polymorphs crystallizing in the same space group. *Dalton Trans* **2020**, *49*, 8443−8447.

(5) Ok, K. M.; Halasyamani, P. S. New Metal Iodates: Syntheses, Structures, and Characterizations of Noncentrosymmetric $La(IO_3)_3$ and $NaYI_4O_{12}$ and Centrosymmetric ß-$Cs_2I_4O_{11}$ and $Rb_2I_6O_{15}(OH)_2\cdot H_2O$. *Inorg. Chem.* **2005**, *44*, 9353−9359.

(6) Ok, K. M.; Halasyamani, P. S. The Lone-Pair Cation I^{5+} in a Hexagonal Tungsten Oxide-Like Framework: Synthesis, Structure, and Second-Harmonic Generating Properties of $Cs_2I_4O_{11}$. *Angew. Chem.* **2004**, *116*, 5605−5607.

(7) Sun, C. F.; Hu, C. L.; Kong, F.; Yang, B. P.; Mao, J. G. Syntheses and crystal structures of four new silver(I) iodates with d^0-transition metal cations. *Dalton Trans* **2010**, *39*, 1473−1479.

(8) Kim, Y. H.; Tran, T. T.; Halasyamani, P. S.; Ok, K. M. Macroscopic polarity control with alkali metal cation size and coordination environment in a series of tin iodates. *Inorg. Chem. Front.* **2015**, *2*, 361−368.

(9) Xu, X.; Yang, B. P.; Huang, C.; Mao, J. G. Explorations of New Second-Order Nonlinear Optical Materials in the Ternary Rubidium Iodate System: Noncentrosymmetric ß-$RbIO_3(HIO_3)_2$ and Centrosymmetric $Rb_3(IO_3)_3(I_2O_5)(HIO_3)_4(H_2O)$. *Inorg. Chem.* **2014**, *53*, 1756−1763.

(10) Abudouwufu, T.; Zhang, M.; Cheng, S. C.; Zeng, H.; Yang, Z. H.; Pan, S. L. $K_2Na(IO_3)_2(I_3O_8)$ with Strong Second Harmonic Generation Response Activated by Two Types of Isolated Iodate Anions. *Chem. Mater.* **2020**, *32*, 3608−3614.

(11) Liu, H. M.; Jiang, X. X.; Wang, X. X.; Yang, L.; Lin, Z. S.; Hu, Z. G.; Meng, X. G.; Chen, X. G.; Qin, J. G. Influence of A-site Cations on Germanium Iodates as Mid-IR Nonlinear Optical Materials: $A_2Ge(IO_3)_6$ (A = Li, K, Rb and Cs) and $BaGe(IO_3)_6H_2O$. *J. Mater. Chem. C* **2018**, *6*, 4698−4705.

(12) Gai, M. Q.; Tong, T. H.; Wang, Y.; Yang, Z. H.; Pan, S. L. New Alkaline-Earth Metal Fluoroiodates Exhibiting Large Birefringence and Short Ultraviolet Cutoff Edge with Highly Polarizable $(IO_3F)^{2-}$ Units. *Chem. Mater.* **2020**, *32*, 5723−5728.

(13) Hermet, P. First-principles based analysis of the piezoelectric response in a-$LiIO_3$. *Comput. Mater. Sci.* **2017**, *138*, 199−203.

(14) Huang, H. W.; He, Y.; Guo, Y. X.; He, R.; Lin, Z. S.; Zhang, Y. H. Hydrothermal synthesis, nonlinear optical property and photocatalytic activity of a non-centrosymmetric $AgIO_3$ photocatalyst under UV and visible light irradiation. *Solid State Sci.* **2015**, *46*, 37−42.
(15) Zhang, J.; Du, X. H.; Ke, S. H.; Xu, B.; Zheng, G. H.; Rowlands, D. A.; Yao, K. L. Dielectric, piezoelectric and nonlinear optical properties of polar iodate $BiO(IO_3)$ from first-principles studies. *J. Solid State Chem.* **2020**, *281*, 121057.
(16) Chen, J.; Hu, C. L.; Mao, F. F.; Zhang, X. H.; Yang, B. P.; Mao, J. G. $LiMg(IO_3)_3$: an excellent SHG material designed by single-site aliovalent substitution. *Chem. Sci.* **2019**, *10*, 10870−10875.
(17) Fan, H. X.; Lin, C. S.; Chen, K. C.; Peng, G.; Li, B. X.; Zhang, G.; Long, X. F.; Ye, N. $(NH_4)Bi_2(IO_3)_2F_5$: An Unusual Ammonium-Containing Metal Iodate Fluoride Showing Strong Second Harmonic Generation Response and Thermochromic Behavior. *Angew. Chem., Int. Ed.* **2020**, *59*, 5268−5272.
(18) Liu, H. M.; Wu, Q.; Jiang, X. X.; Lin, Z. S.; Meng, X. G.; Chen, X. G.; Qin, J. G. $ABi_2(IO_3)_2F_5$ (A = K, Rb, and Cs): A Combination of Halide and Oxide Anionic Units To Create a Large Second-Harmonic Generation Response with a Wide Bandgap. *Angew. Chem., Int. Ed.* **2017**, *56*, 9492−9496.
(19) Huang, H. W.; He, Y.; He, R.; Lin, Z. S.; Zhang, Y. H.; Wang, S. C. Y. $(IO_3)_3$ as a Novel Photocatalyst: Synthesis, Characterization, and Highly Efficient Photocatalytic Activity. *Inorg. Chem.* **2014**, *53*, 8114−8119.
(20) Gai, M. Q.; Wang, Y.; Tong, T. H.; Yang, Z. H.; Pan, S. L. $ZnIO_3F$: Zinc Iodate Fluoride with Large Birefringence and Wide Band Gap. *Inorg. Chem.* **2020**, *59*, 4172−4175.
(21) Cao, L. L.; Luo, M.; Lin, C. S.; Zhou, Y. Q.; Zhao, D.; Yan, T.; Ye, N. From centrosymmetric to noncentrosymmetric: intriguing structure evolution in d^{10}-transition metal iodate fluorides. *Chem. Commun.* **2020**, *56*, 10734−10737.
(22) Jia, Y. J.; Chen, Y. G.; Guo, Y.; Guan, X. F.; Li, C. B.; Li, B. X.; Liu, M. M.; Zhang, X. M. $LiM^{II}(IO_3)_3$ (M^{II} = Zn and Cd): Two Promising Nonlinear Optical Crystals Derived from a Tunable Structure Model of a-$LiIO_3$. *Angew. Chem., Int. Ed.* **2019**, *58*, 17194−17198.
(23) Liu, A. J.; Xu, F.; Han, S. D.; Pan, J.; Wang, G. M. Mixed-Ligand Strategy for the Construction of Photochromic Metal−Organic Frameworks Driven by Electron-Transfer Between Non-photoactive Units. *Cryst. Growth Des.* **2020**, *20*, 7350−7355.
(24) Bai, Z. Y.; Hu, C. L.; Wang, D. M.; Liu, L. H.; Zhang, L. Z.; Huang, Y. S.; Yuan, F. F.; Lin, Z. B. $[Al(H_2O)_6](IO_3)_2(NO_3)$: a material with enhanced birefringence induced by synergism of two superior functional motifs. *Chem. Commun.* **2020**, *56*, 11629−11632.
(25) Zhang, M.; An, D. H.; Hu, C.; Chen, X. L.; Yang, Z. H.; Pan, S. L. Rational Design via Synergistic Combination Leads to an Outstanding Deep-Ultraviolet Birefringent $Li_2Na_2B_2O_5$ Material with Unvalued B_2O_5 Functional Gene. *J. Am. Chem. Soc.* **2019**, *141*, 3258−3264.
(26) Shin, W. H.; Roh, J. W.; Ryu, B.; Chang, H. J.; Kim, H. S.; Lee, S.; Seo, W. S.; Ahn, K. Enhancing Thermoelectric Performances of Bismuth Antimony Telluride via Synergistic Combination of Multi-scale Structuring and Band Alignment by $FeTe_2$ Incorporation. *ACS Appl. Mater. Interfaces* **2018**, *10*, 3689−3698.
(27) Ok, K. M. Functional layered materials with heavy metal lone pair cations, Pb^{2+}, Bi^{3+}, and Te^{4+}. *Chem. Commun.* **2019**, *55*, 12737−12748.
(28) Mao, F. F.; Hu, C. L.; Xu, X.; Yan, D.; Yang, B. P.; Mao, J. G. $Bi(IO_3)F_2$:The First Metal Iodate Fluoride with a Very Strong Second Harmonic Generation Effect. *Angew. Chem., Int. Ed.* **2017**, *56*, 2151−2155.
(29) Phanon, D.; Suffren, Y.; Taouti, M. B.; Benbertal, D.; Brenier, A.; Gautier-Luneau, I. Optical properties of Nd^{3+} and Yb^{3+}-doped $AgM(IO_3)_4$ metal iodates: transparent host matrices for mid-IR lasers and nonlinear materials. *J. Mater. Chem. C* **2014**, *2*, 2715−2723.
(30) Cao, Z. B.; Yue, Y. C.; Yao, J. Y.; Lin, Z. S.; He, R.; Hu, Z. G. $Bi_2(IO_4)(IO_3)_3$: A New Potential Infrared Nonlinear Optical Material Containing $[IO_4]^{3-}$ Anion. *Inorg. Chem.* **2011**, *50*, 12818−12822.
(31) Chen, F.; Ma, Z. Y.; Ye, L. Q.; Ma, T. Y.; Zhang, T. R.; Zhang, Y. H.; Huang, H. W. Macroscopic Spontaneous Polarization and Surface Oxygen Vacancies Collaboratively Boosting CO_2 Photoreduction on $BiOIO_3$ Single Crystals. *Adv. Mater.* **2020**, *32*, 1908350.
(32) Huang, H. W.; Chen, F.; Reshak, A. H.; Auluck, S.; Zhang, Y. H. Insight into crystal-structure dependent charge separation and photo-redox catalysis: A combined experimental and theoretical study on $Bi(IO_3)_3$ and $BiOIO_3$. *Appl. Surf. Sci.* **2018**, *458*, 129−138.
(33) Nguyen, S. D.; Yeon, J.; Kim, S. H.; Halasyamani, P. S. $BiO(IO_3)$: A New Polar Iodate that Exhibits an Aurivillius-Type $(Bi_2O_2)^{2+}$ Layer and a Large SHG Response. *J. Am. Chem. Soc.* **2011**, *133*, 12422−12425.
(34) Zhang, L. L.; Tang, Y. L.; Khan, A. R.; Hasan, M. M.; Wang, P.; Yan, H.; Yildirim, T.; Torres, J. F.; Neupane, G. P.; Zhang, Y. P.; Li, Q.; Lu, Y. R. 2D Materials and Heterostructures at Extreme Pressure. *Adv. Sci.* **2020**, *7*, 2002697.
(35) Wen, T.; Wang, Y. G.; Li, N. N.; Zhang, Q.; Zhao, Y. S.; Yang, W. G.; Zhao, Y. S.; Mao, H. K. Pressure-Driven Reversible Switching between n- and p-Type Conduction in Chalcopyrite $CuFeS_2$. *J. Am. Chem. Soc.* **2019**, *141*, 505−510.
(36) Wang, Y. Q.; Guo, S. H.; Luo, H.; Zhou, C. K.; Lin, H. R.; Ma, X. D.; Hu, Q. Y.; Du, M. H.; Ma, B. W.; Yang, W. G.; Lü, X. J. Reaching 90% Photoluminescence Quantum Yield in One Dimensional Metal Halide $C_4N_2H_{14}PbBr_4$ by Pressure-Suppressed Nonradiative Loss. *J. Am. Chem. Soc.* **2020**, *142*, 16001−16006.
(37) Li, Q.; Chen, Z. W.; Yang, B.; Tan, L.; Xu, B.; Han, J.; Zhao, Y. S.; Tang, J.; Quan, Z. W. Pressure-Induced Remarkable Enhancement of Self-Trapped Exciton Emission in One-Dimensional $CsCu_2I_3$ with Tetrahedral Units. *J. Am. Chem. Soc.* **2020**, *142*, 1786−1791.
(38) Ji, C.; Li, B.; Liu, W. J.; Smith, J. S.; Majumdar, A.; Luo, W.; Ahuja, R.; Shu, J. F.; Wang, J. Y.; Sinogeikin, S.; Meng, Y.; Prakapenka, V. B.; Greenberg, E.; Xu, R. Q.; Huang, X. R.; Yang, W. G.; Shen, G. Y.; Mao, W. L.; Mao, H. K. Ultrahigh-pressure isostructural electronic transitions in hydrogen. *Nature* **2019**, *573*, 558−562.
(39) Mao, H. K.; Chen, X. J.; Ding, Y.; Li, B.; Wang, L. Solids, liquids, and gases under high pressure. *Rev. Mod. Phys.* **2018**, *90*, 015007.
(40) Mao, H. K.; Chen, B.; Chen, J. H.; Li, K.; Lin, J. F.; Yang, W. G.; Zheng, H. Y. Recent advances in high-pressure science and technology. *Matter Radiat. Extremes* **2016**, *1*, 59−75.
(41) Zhang, W. W.; Cui, Q. L.; Pan, Y. W.; Dong, S. S.; Liu, J.; Zou, G. T. High-pressure x-ray diffraction study of $LiIO_3$ to 75 GPa. *J. Phys.: Condens. Matter* **2002**, *14*, 10579−10582.
(42) Bayarjargal, L.; Wiehl, L.; Friedrich, A.; Winkler, B.; Juarez-Arellano, E. A.; Morgenroth, W.; Haussuhl, E. Phase transitions in KIO_3. *J. Phys.: Condens. Matter* **2012**, *24*, 325401−325411.
(43) Suffren, Y.; Gautier-Luneau, I.; Darie, C.; Goujon, C.; Legendre, M.; Leynaud, O. First Evidence of a Phase Transition in a High-Pressure Metal Iodate: Structural and Thermal Studies of $AgIO_3$ Polymorphs. *Eur. J. Inorg. Chem.* **2013**, *2013*, 3526−3532.
(44) Liang, A.; Rahman, S.; Saqib, H.; Rodriguez-Hernandez, P.; Muñoz, A.; Nénert, G.; Yousef, I.; Popescu, C.; Errandonea, D. First-Order Isostructural Phase Transition Induced by High Pressure in $Fe(IO_3)_3$. *J. Phys. Chem. C* **2020**, *124*, 8669−8679.
(45) Liang, A.; Rahman, S.; Rodriguez-Hernandez, P.; Muñoz, A.; Manjón, F. J.; Nenert, G.; Errandonea, D. High-Pressure Raman Study of $Fe(IO_3)_3$: Soft-Mode Behavior Driven by Coordination Changes of Iodine Atoms. *J. Phys. Chem. C* **2020**, *124*, 21329−21337.
(46) Brese, N. E.; O'Keeffe, M. Bond-Valence Parameters for Solids. *Acta Crystallogr., Sect. B: Struct. Sci.* **1991**, *B47*, 192−197.
(47) Bentria, B.; Benbertal, D.; Bagieu-Beucher, M.; Masse, R.; Mosset, A. Crystal structure of anhydrous bismuth iodate, $Bi(IO_3)_3$. *J. Chem. Crystallogr.* **2003**, *33*, 867−873.
(48) Jia, Y. J.; Chen, Y. G.; Wang, T.; Guo, Y.; Guan, X. F.; Zhang, X. M. $KBi(IO_3)_3(OH)$ and $NaBi(IO_3)_4$: from the centrosymmetric chain to a noncentrosymmetric double layer. *Dalton Trans* **2019**, *48*, 10320−10326.

https://dx.doi.org/10.1021/acs.inorgchem.0c03697
Inorg. Chem. 2021, 60, 2893−2898

(49) Huang, Y.; Meng, X. G.; Gong, P. F.; Yang, L.; Lin, Z. S.; Chen, X. G.; Qin, J. G. $A_2BiI_5O_{15}$ (A = K^+ or Rb^+): two new promising nonlinear optical materials containing $[I_3O_9]^{3-}$ bridging anionic groups. *J. Mater. Chem. C* **2014**, *2*, 4057−4062.

https://dx.doi.org/10.1021/acs.inorgchem.0c03697
Inorg. Chem. 2021, 60, 2893−2898